

Design Methodology Based on H_∞ Control Theory for Marine Propulsion System with Bumpless Transfer Function

M. J. LOPEZ, L. GARCIA, J. LORENZO, A. CONSEGLIERE

Departamento de Ingeniería de Sistemas y Automática

Universidad de Cádiz

Centro Andaluz Superior Estudios Marinos (CASEM)

SPAIN

{manueljesus.lopez, luis.garcia, jose.lorenzo, agustin.consegliere}@uca.es

<http://www2.uca.es/dept/isa-tee/>

Abstract: - In this paper we propose a control system design methodology which has two main objectives: the first one is to achieve control system specifications for a local H_∞ controller designed for a given operation condition, and the second objective is to provide a procedure for bumpless transfer (BLT) when the controller is switched to another one, due to change in the operation condition, or when the controller is retuned by a plant operator. For that, the design procedure calculates a feedback H-controller (FB-HC) and an associated bump-less transfer H-controller (BLT-HC). The method is implemented in an auto-tuning procedure, where both pre-tuning controllers (FB-HC and BLT-HC) are obtained in a systematic manner. Controllers fine-tuning can be carried out by a plant operator using two tuning parameters and several tuning rules. Our design methodology is applied to a marine propulsion system with diesel engine used as propeller prime-mover. Due to different operation regimens of ship propulsion, several linear controllers are designed for different operating points, switching (with bumpless-transfer) between them when is necessary; which enables the system to be controlled satisfactorily within the whole of its operating range. Satisfactory results are obtained by simulations with the nonlinear model of a merchant ship, and our hardware in the loop simulation (HILS) environment is described.

Key-Words: - ship propulsion system, H controller, bumpless transfer

1 Introduction

When a controller is designed and implemented for an industrial or marine process, on-line changes in controller are required to adapt control system to new situations [1,2,3,4,5]. The problem of bumpless transfer refers to the instantaneous switching between two controllers of a process while retaining a smooth ("bumpless") control signal. Avoiding transients after switching from a controller to other one can be viewed as an initial condition problem on the output of the feedback controller. In process control and marine systems there are several practical situations that may all be interpreted as bumpless transfer problems. These are:

1. Switching between manual and automatic control. The ability to switch between manual and automatic control while retaining a smooth control signal is the traditional bumpless transfer problem.
2. Controller tuning. It is frequently desired to tune controller parameters on-line and in response to experimental observations.
3. Scheduled and adaptive controllers. Scheduled controllers are controllers with time-varying parameters. These time variations are usually due to

measured time-varying process parameters or due to local linearization in different operating ranges.

4. Tentative evaluation of new controllers. This is a challenging, and only recently highlighted bumpless transfer scenario. It is motivated by the need to test tentative controller designs safely and economically on industrial and marine processes during normal operation.

Consider, for example, a process operating in closed loop with an existing controller. Assume that the performance is unsatisfactory, and that a number of new controller candidates have been designed and simulated. It is then desired to test these controllers, tentatively, on the plant to assess their respective performances. Frequently it is not possible or feasible to shut down the plant intermittently, and the alternative controllers therefore have to be brought on-line with a bumpless transfer mechanism during normal plant operation.

Controller design for marine systems are mainly based on PID technology [1,2,3,4,5,6], nevertheless, if advanced control strategies are used, some improved results can be obtained. In this work we propose a method based on H_∞ control theory, which is complemented with a method for bumpless transfer

(BLT) when controller switching is needed. The method for BLT is also based on H_∞ control theory, but it is applied to PID controllers. Our design methodology for controller design and BLT is proved by means of simulation tests with the propulsion system of a merchant ship.

Diesel engine is used as propeller prime-mover for the majority of modern merchant ships. This is due to three major reasons: 1) the superior (thermal) efficiency of Diesel engines, b) large Diesel engines can burn heavy fuel oil (HFO), c) slow-speed Diesel engines can be directly connected to the propeller without the need of gearbox and/or clutch and are reversible. As shortcoming, Diesel engines require a large engine room compared to gas turbines, which can be a problem when extremely large power outputs are required for large high-speed vessels [1,2].

In this work, robust control theory results are applied to design the propulsion control system of a merchant ship. We employ a mathematical model which is a synthesis of different models given in literature [1,2,3,4,5,6], a nonlinear model which captures the essential characteristics of ship propulsion dynamics and it is used in order to carry out real time hardware in the loop simulations (HILS) [7,8,9,10]. Linearized models are used to design PID and H_∞ controllers [1,2,3,4,10,11,12] for different operation conditions. To change controller parameters without bump effect we propose a bump-less procedure, which is applicable for controller switching in gain scheduling method used for adapting controller to changes in plant dynamics.

The rest of this paper is organized as follows: in section two the system propulsion model is described, the controller design methodology is outlined in section three, simulation results are depicted in section four, and finally concluding remarks are given in section five.

2 Propulsion system model

The propulsion system consists of two basic control loops, one for propeller pitch (pitch controller) and one for shaft speed (shaft speed controller). The propulsion set-point is performed by a lever, named "the telegraph", placed on the bridge. Each lever position corresponds, via the combinatory curve, to a pitch setting and to the required rotational speed of the engine. The reference signals are then transmitted to the controller (named governor). The governor inputs are the requested (set-point) and the actual engine speeds, as well as the propeller pitch and its set-point are used. The governor controls the fuel flow to the cylinders in order to maintain the required engine speed (see Fig.1).

Diesel engine of the prime-mover is modelled taking into account the following components (see block diagram of Fig. 1, where the basic signals and elements of the control system are shown): 1) the input signal produced by the controller (controller output, CO) is first converted to an equivalent current signal that drives the actuator. The injection actuator has a time constant τ_a (as nominal value $\tau_a = 0.1$ sec. is used in simulations) that is dependent on the oil temperature. The output of this unit is the fuel-flow, which is a direct input to the engine. The injection process is characterised by a dead-time (injection delay) τ_d , which is a non-linear function of the engine speed [1,2,3,14]

$$\tau_d = (AN^2 + BN + C)/N^2$$

which has been estimated to lie within the range:

$$15/N < \tau_d < 15/N + 60/(Nz)$$

where z is the number of engine cylinders.

To model the engine thermodynamic process that determines engine brake torque Q_{eng} (manipulated variable, MV in Fig. 1), a first order transfer function with thermodynamic gain K_{TC} and time constant τ_{TC} is considered [2,3,4]

$$\tau_{TC} \dot{Q}_{eng}(t) + Q_{eng}(t) = K_{TC} F_R(t - \tau_d)$$

where F_R is the named fuel index (rack) position or fuel-rack position, in this equation τ_{TC} is mainly due to the effect of turbo-charging on the power generation process. As nominal value it is used $\tau_{TC} = 0.25$ seconds in simulations. Propeller thrust T_p and torque Q_p are modelled by means of

$$T_p = K_T N^2 |\theta| \theta$$

$$Q_p = K_Q N^2 |\theta| \theta$$

where θ is the propeller pitch ratio, K_T and K_Q vary with propeller shaft-speed N (process variable, PV in Fig. 1), and advance velocity V_a , and can be approximated as a n -th order polynomial in advance number J_a . Usually, a first order polynomial

$$K_Q = K_{Q0} + K_{Q1} J_a, \quad J_a = V_a / (ND)$$

$$K_T = K_{T0} + K_{T1} J_a$$

or second order polynomial are employed [15,16,17,18], where D is the propeller diameter, and advance velocity V_a of the water-flow over the

propeller disk is related to the ship's surge velocity U via wake coefficient w , as $V_a = (1-w)U$.

In practice, K_Q and K_T undergo fluctuations due to variations on shaft rpm and ship surge speed, and this must be taken into account in the design procedure for robust controller. In this context, variations on K_Q and on K_T can be treated as disturbances acting on the

where Q_{eng} is the engine torque, Q_p is the propeller demand torque and Q_{ext} is used to take into account external disturbances.

To take into account waves induced disturbance, which produces a variation in propeller torque, it is used an approximation of the Pierson and Moscowitz spectrum, what is common in the field of marine

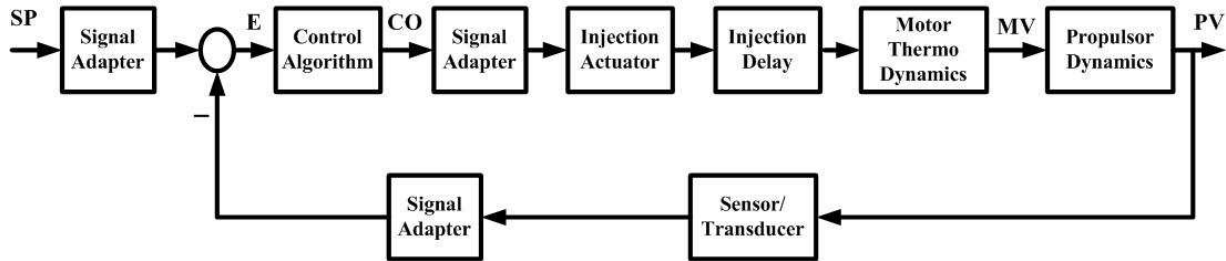


Fig. 1. Elements of the Propulsion Control Marine System

process instead of considering uncertain parameters. In this work, we limit our study to variations on K_Q parameter only. Fluctuations on K_Q is one of the major disturbance to marine plant operation and the source of perturbations for the engine rpm $N(t)$ and fuel index $F_R(t)$ signals. For a nominal operation condition with θ_{nom} , N_{nom} and K_{Qnom} as nominal values, if a linear approximation is made, a variation in K_Q of magnitude ΔK_Q supposes a disturbance acting on system which is equivalent to

$$\Delta Q_p = N_{nom}^2 \theta_{nom} |\theta_{nom}| \Delta K_Q$$

Under this approximation, propeller fluctuations can be simulated using as disturbance an input signal (ΔK_Q), which will be composed by deterministic signals (step, ramp, pulse, sine, exponential, etc.) and stochastic signals (white noise or coloured noise obtained passing white noise through a low pass filter).

The propulsion plant and surge ship dynamics can be represented by two dynamical equations, the first equation represents the surge motion of the ship,

$$M\dot{U} = T_p - T_R$$

where T_R is the ship resistance and M is the effective mass. The second equation represents the rotational motion of the shaft line

$$J\dot{N} = Q_{eng} - Q_p - Q_{ext}$$

control engineering. For that, it is used a second-order model driven by white noise [11,12,13,14]

$$D_w(s) = \frac{\omega_w s}{s^2 + 2\omega_w \xi s + \omega_w^2}$$

where ω_w is the central wave frequency, and $\xi = 0.15$ typically. The output $d(t)$ of the filter $D_w(s)$ is used as the wave induced propeller torque disturbance, and its magnitude depends on the variance of the white noise employed.

In order to controller design and linear analysis, linearization of the system equations are employed for the vessel sailing under service speed conditions, i.e., the nominal (steady-state) operating points. For a concrete ship, it is necessary to carry out towing tank tests and sea trial experiments, and with the acquired data to adjust parameters and improve equations of the mathematical model. Nevertheless, that approach is not objective in this paper and will be carried out in next works with real marine systems in collaboration with a marine construction company.

In real time simulation studies with hardware in the loop (RT-HILS) the differential equations are solved using fourth order Runge-Kutta method with fixed step size of 1.0 ms. The dead-time is implemented using a circular buffer using the same step time. For RT-HILS we employ EPESC hardware/software environment [9,10].

3 Controller design methodology

The success and widespread use of linear design techniques in control system design can, in part, be attributed to the relative ease of synthesis and

implementation of linear controllers, and to the powerful, intuitive and convenient mathematics associated with linear systems theory [16,17,18]. However, the strengths of these techniques have to be balanced against the fact that all real-world systems are, to some varying degrees, inherently non-linear. This has the consequence that most linear controllers have to be designed around a specific operating point. Variation around this operating point can cause degradation of the performance of the controlled system, even when the engineer employs robust methods of design.

Due to different regimens operation of ship propulsion, it is common practice to design more than one linear controller, each at a different operating point, and to switch between them; which enables the system to be controlled satisfactorily within the whole of its operating range.

The problem of smooth real-time switching between controllers, in the closed-loop control applications, is referred as bump-less transfer (BLT). In general, BLT arises in many cases of practical interest. One of such cases is on-line performance assessment of advanced control laws against the industry standard, typically PID-based. Another case is the attainment of an improved closed-loop system performance via switching between the controllers with the complementary properties, such as the ones separately optimized for tracking and disturbance rejection and/or for the specific set-points to cover the entire operating range of interest. In practice, due to controllers are implemented in software, all their states are available, and bump-less transfer is performed in the steady state to meet safety requirements.

In this paper we propose a design methodology for: 1) feedback H-controller (FB-HC) design, 2) bump-less transfer H-controller (BLT-HC) design. For each FB-HC design, it is obtained its corresponding BLT-HC as it is shown in Fig. 1; where: GcA represents the active FB-HC, GcL corresponds to the latent FB-HC, and GcBLT represents the BLT-HC.

The proposed methodology in this paper for H-controller design procedure is given below. It is carried out in automatic form (auto-tuning), and the user does not need to know theoretical fundamentals of H control, only needs to know how to adjust two parameters ρ_H and β_H . A third parameter (σ_H) is fixed to a constant value. In Fig. 2 the Simulink realization of the propulsion control system is given. Simulink and Matlab [19] are used in the first phase of simulation, controller design and control system analysis. Once satisfactory results have been obtained, real time simulations with hardware in the

loop will be carried out. As it can be seen in Fig. 2, H_∞ controller and PID controller have been considered. A fine tuning PID controller is used in order to compare with H-controller. For pre-tuning PID parameters different methods are available in literature [20]. In our case, we have employed methods based on the reaction curve of the process (response to a step change in control signal), which use a first order plus dead time (FOPDT). Specifically, we have employed PI and PID controllers which minimize the IAET (Integral Absolute Error Time) for step changes in setpoint or for load changes according to the case to solve [20].

FB-HC design.

The following steps are followed in order to design the H_∞ controller for process control (ship propulsion):

Step 1. It is used a model of the plant for controller design, $G_H(s)$. This is obtained from experimental identification, or by linearization in case of the non-linear model of the process be known.

Step 2. It is obtained two parameters associated to plant dynamics: K_H and τ_H . For ship propulsion control, K_H coincides with stationary gain, and τ_H is the effective time constant.

Step 3. Weighting transfer functions

$$\{W_S(w, \tau_H, \rho_H), W_R(\beta_H), W_T(\sigma_H)\}$$

are calculated using pre-tuning values for adjusting parameters ρ_H and β_H .

The meaning of each weighting transfer function is as follows: $W_S(w, \tau_H, \rho_H)$ (first order transfer function) is used in order to fix closed loop bandwidth and depends on angular frequency w ; $W_R(\beta_H)$ (zero order transfer function) takes into account control effort, and $W_T(\sigma_H)$ (zero order transfer function) is related with relative uncertainty bound at low frequencies.

Step 4. It is used zero order hold (ZOH) transformation for $G_H(s)$ discretization, with sampling time T_m , $G_H(z)$.

Step 5. Inverse bilinear transform is used for w -plane transfer function $G_H(w)$.

Step 6. It is obtained the generalized plant $P_H(w)$.

Step 7. It is solved the following H_∞ optimal problem

$$\|T_{zw}(w)\|_\infty < \gamma, \quad \gamma > 0$$

and H-controller is obtained $Gc(w)$, where

$$T_{zw} = [W_S S \quad W_R R \quad W_T T]^T$$

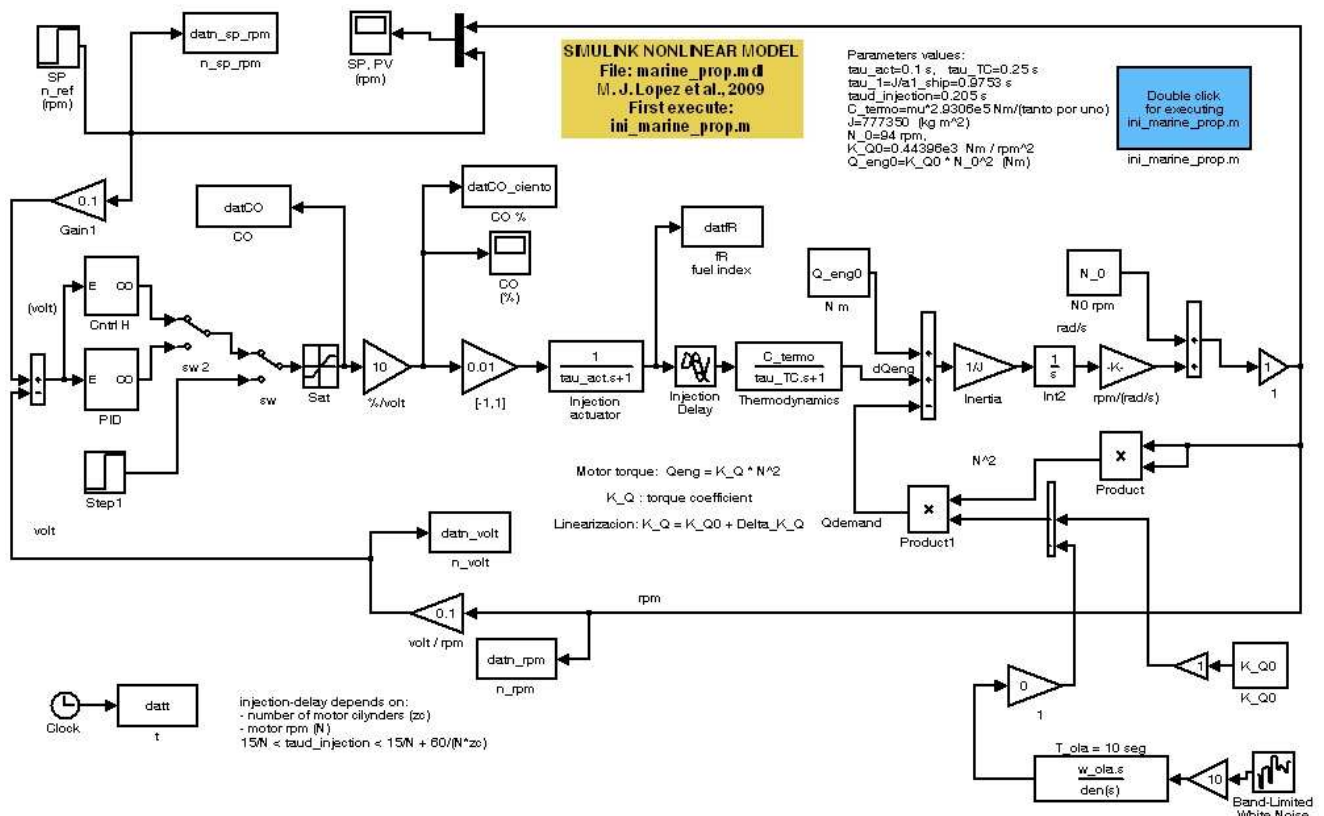


Fig. 2. Simulink realization of the propulsion control system (first phase in design and analysis procedure)

Step 8. Bilinear transform is used for obtaining discrete version of the controller, $G_c(z)$. This controller is implemented as a recursive algorithm.

Step 9. Performance and robustness of the control system are analyzed using numerical indicators obtained with G_c and G_H in first phase, and with actual process in second phase (for fine tuning controller). If performance and robustness indicators (PRI) are satisfactory then finish the design procedure and go to step 10; in other case, modify fine tuning parameters (ρ_H , β_H) and go to step 3.

Step 10. Finish design procedure for the feedback H-controller (FB-HC).

In case of auto-tuning method, steps 1 to 8 are carried out in an automatic procedure, where the model of the system is obtained from identification test of the process to control. In this case, the obtained controller is named "auto-tuned controller". A fine-tuning procedure is employed if it is necessary, and it is carried out by a plant operator. For that, plant operator must take into account several expert rules, which consider several basic performance parameters: overshoot (M_p), rise time (t_r), controller effort related with control signal

intensity (CSI), robustness properties (gain margin, MG, and phase margin, MF).

Rule 1. If M_p is high, then reduce ρ_H .

Rule 2. If t_s is high, then increase ρ_H .

Rule 3. To maintain practically constant M_p and t_s and to reduce CSI, increase β_H .

Rule 4. In order to increase robustness properties MG, MF), reduce ρ_H and/or increase β_H .

With these four rules a plant operator will be able to carry out the H-controller fine-tuning, but this plant operator does not need to know anything about H-infinity robust control theory, he only needs to know what parameters must adjust to achieve the desired effect over the control system. This is an innovative difference and important property of our proposal, due to all complicated methods and calculations related with H-infinity control theory is transparent for the plant operator. This is possible due to the computer application ControlAvH Tune [21,22], which implements the methods and computations and facilitates the interface with the user or plant operator.

Other two basic considerations to take into account are: 1) If satisfactory M_p and t_r are obtained but the

settling time (t_s) is too much high, this may be adjusted using the combination of controller parameters, ρ_H and β_H . 2) The stationary error (e_{ss}) for step changes in setpoint and for load changes or disturbances is guaranteed to be zero due to integral action in H controller.

Once the FB-HC has been obtained, the BLT-HC is calculated using the FB-HC controller as process to control. In this form, each FB-HC has associated a BLT-HC, which is turned on during a time interval (Δt_1) previous to the instant when the FB-HC is set as the active controller, and is turned off a time interval (Δt_2) later to the instant when the FB-HC is set as the active controller (see Fig. 2). Every time the active controller is going to change, this operation is carried out.

BLT-HC design

For the bump-less transfer H-controller (BLT-HC) design, a similar procedure is followed, but in this case the feedback H-controller (FB-HC) is used as process to control. In Fig. 1, GcA is the active controller, GcL is the latent controller and GcBLT is the BLT controller designed for GcL. Therefore, GcL is used as plant for GcBLT design. The BLT-HC design procedure is applied even if the GcL is a PID type controller. In this case, PID would be used as plant model for the GcBLT calculation.

In this context, we consider two controllers associated to each considered design condition. One of this controllers corresponds to the feedback controller for process to control (FB-HC), in our case, the controller designed for the propulsion control system.

The other design corresponds to the BLT controller (BLT-HC), which is designed once the FB-HC has been obtained, due to the FB-HC is used as model or process for controller design. As it can be seen in Fig. 1, GcBLT (FB-HC) is controlled by GcL (BLT-HC), so that the output of GcBLT (u_L) follows to the output (u_A) of the active controller, GcA. In this case, u_A is the setpoint for GcL-GcBLT loop.

If the three controllers, GcA, GcL and GcBLT, are simultaneously running, when the switching between controllers happens, the transition is made with bumpless transfer (BLT). Nevertheless, it is not necessary to hold the three controllers running all the time, only it is necessary to have running GcL and GcBLT a time previously to switch operation from active controller GcA to latent controller GcL. This time is used for achieving that GcL output follows the GcA output, in other case, bump effect will happen.

If a PID (PI) controller is compared with a H-controller, from the point of view of difficulty to

carry out the design, it is obviously decided that PID is much easier than H-controller. Nevertheless, the difficulty must be considered as something relative, since if computation are transparent for the user, and there are similar rules to adjust controllers, then from the point of view of a plant operator will be very similar to use PID or H-controller.

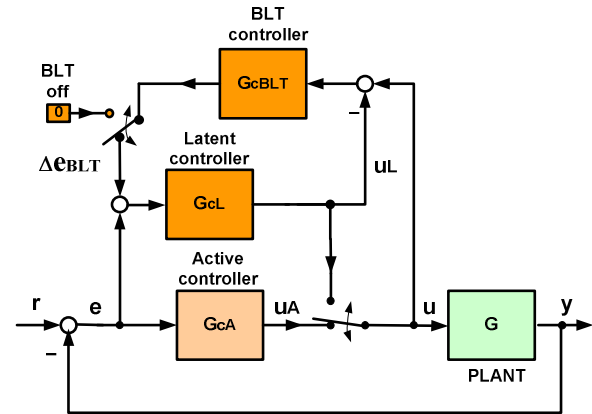


Fig. 3. Structure for switching between controllers with bump-less transfer controller.

4 Simulation results

In order to have plants simulated in real time with hardware in the loop support for testing controller designs for different marine control systems (such as heading control, rolling attenuation and propulsion control), we have been using mathematical models based on different references [2,3,4,12,13,14,15]. In this paper we present results obtained with adapted data of the SE propulsion system, where additionally transducers from rpm to volt have been included and variable pitch propeller have been considered. Nevertheless, only the control loop of propeller rpm (N) has been designed and analyzed, meanwhile propeller pitch control dynamics is given by

$$\frac{\theta(s)}{\theta_{SP}(s)} = \frac{K_\theta}{s + K_\theta}$$

where θ_{SP} is the demanded propeller pitch or setpoint, and θ is the actual propeller pitch.

The propulsion power plant of the containership “Shanghai Express” (SE) is considered as a typical case of a merchant ship propulsion system [2]. In this case, illustrative data of propeller speeds are given (for fixed pitch propeller): for fuel index (F_R) of 25% propeller rotational speed (N) is 59.2 rpm, for $F_R = 50\%$, 75% and 100%, the following speeds are respectively obtained: $N = 74.6$ rpm, 85.4 rpm and 94.0 rpm.

For a given plant condition, the linearized model has the following form:

$$G(s) = \frac{KKg}{(\tau_{TC}s + 1)(\tau_a s + 1)(\tau_p s + 1)} \exp(-\tau_d s)$$

For nominal operation ($F_R = 75\%$ and $N = 85.4$ rpm, $Kg = 1$) is given by

$$G(s) = \frac{43.201}{(s + 10)(s + 4)(s + 1.025)} \exp(-0.21s)$$

$G(s)$ relates rpm of the ship propeller expressed in volts (output of rpm transducer) with the controller signal in volts (input to injection actuator). This response is used for system identification and the following estimated model (first order plus dead time, FOPDT) is obtained. This model is used in practice for PID tuning.

$$\hat{G}_{FOPDT}(s) = \frac{1.052}{1.05s + 1} \exp(-0.52s)$$

FOPDT and linearized models are used for controller design, and the obtained results with PID and H_∞ controller are analyzed with the nonlinear model described before. For controller design, dead time term is approximated as a first order Padé approximation. Advantages of H_∞ controller are basically: 1) easy to design using our procedure implemented in ControlAvH software [21,22], b) our fine tuning procedure only depends on two parameters (ρ_H, β_H) and it is based on basic rules, c) control system performance and robustness are improved with respect to PID. Classical drawbacks associated with H_∞ control, such as difficult of the design procedure and high order or the controller are overcome. On one hand, this is due to the fact that a digital fourth/fifth order controller is easy to implement in hard real time for specific digital processors (such as microcontrollers or digital signal processors, DSP), for Programmable Automation Controller (PAC) such as the provided by NI [23] and also for an industrial programmable automata or PLC (in case of recursive algorithms or difference equations can be implemented in the software of the respective PLC of new generation); and for the other side, the design procedure is transparent for the user, due to he only must take into account the relation between two design parameters (ρ_H, β_H) and its relation with the control system observed response. No theoretical knowledge about H_∞ control is needed for controller fine tuning.

In Fig. 4, closed-loop system responses for three operation conditions (nominal and two others with

$\pm 50\%$ changes in stationary gain for the plant) and a fixed H-controller (designed for $Kg=1$) are shown. These conditions corresponds to changes in stationary gain characterized by Kg parameter, which takes three values: $Kg = 1, 1.5$ and 0.5 . Nevertheless, as it can be seen, one response is so slow (for $Kg = 0.5$), and other has excessive overshoot (for $Kg = 1.5$). Therefore, three controllers (Gc1, Gc2 and Gc3) must be designed, one for each plant operation condition. In this case, satisfactory responses (extremely similar behavior) are also obtained for $Kg = 0.5$ and for $Kg = 1.5$. The used parameters for the three FB-HC designs are the following:

$$\rho_H = 10, \beta_H = 1, \tau_H = 1.05, K_H = 1.052$$

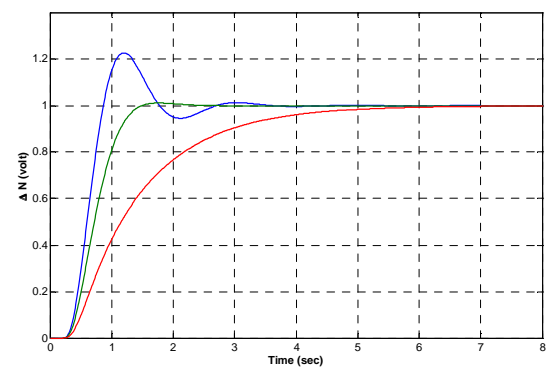


Fig. 4. Closed-loop system responses for three operation conditions ($Kg = 1, 1.5, 0.5$) and a fixed H-controller designed for $Kg = 1$.

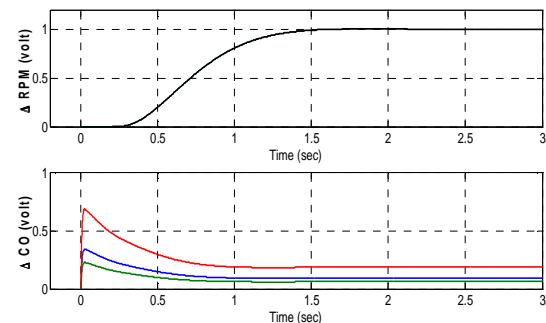


Fig. 5. Closed-loop system responses for three operation conditions ($Kg = 1, 1.5, 0.5$) with their respective H-controllers.

In Fig. 5, the closed-loop system responses for three operation conditions ($Kg = 1, 1.5, 0.5$) and their respective H-controllers (designed for each operation condition) are shown. Practically the same RPM responses are obtained for the three controllers. Due to the proximity between the three RPM responses, it seems that only one curve appears in this Figure.

In order to prove BLT controller the following tests are considered:

Test 1. System is in stationary state with controller designed for $K_g = 1$ (Gc1 as active controller GcA), and it is decided to switch to controller designed for $K_g = 0.5$ (Gc3 as latent controller GcL). If BLT controller is not used, the bump effect happens as it is shown in Figure 6. If BLT is considered, BLT controller can be activated in different instants: a) when it is decided to change the controller from Gc1 to Gc3, b) one half second before to controller switching. If case a) is considered, BLT controller needs a settling time to reduce differences between u_L and u (see Figure 3), and therefore bump effect will not be avoid completely. If case b) is tested, the previous time is used to get that $(u_L - u)$ be sufficiently small and bump-less controller switching is obtained. The following parameters have been used for BLT controller (GcBLT in Figure 3):

$$\rho_H = 0.2, \beta_H = 0.1, \tau_H = 1.05, K_H = 1.052$$

Test 2. In this case, the controller Gc3 (designed for $K_g = 0.5$) is used as plant to control, and the GcBLT is its controller.

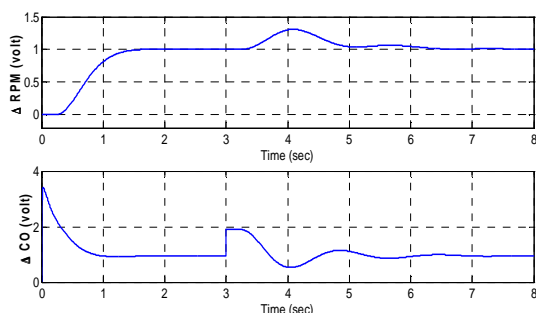


Fig. 6. Closed-loop response for controller switching (Gc1 to Gc3) at $t = 3$ sec., without BLT controller.

Without BLT controller, bump effect is significant as it can be seen in Fig. 6. Resultant effect from switching is an equivalent disturbance. For that, it is employed the BLT controller. In Fig. 5 it can be shown behavior when a BLT (Gc_{BLT} for Gc3) is used. In this case, controller for BLT (Gc_{BLT}) is connected 0.5 sec. before controller switching. This time is necessary for controller convergence: $u_L \rightarrow u$, where u is the actual control signal (from the active controller) and u_L is the signal generated by the latent controller (see Fig. 3).

Hard real time control and simulation

In our laboratory, a Hard Real Time Control and Simulation Environment (EPESC) [9,10] has been developed, for PC-based controllers and PC-based plant simulators; due to PC-based environments are

cheaper than industrial-grade processors and have a more open architecture. This open architecture means

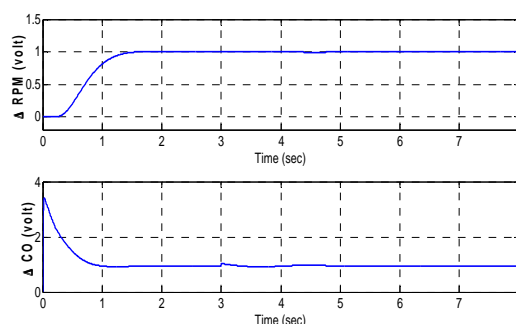


Fig. 7. Bumpless transfer switching from controller Gc1 to controller Gc3 in $t = 3$ sec.

that third-party vendor is able to supply more of the components. Communication between PCs is based on the Ethernet hardware. Low-cost communication suggested the use of TCP/IP or UDP/IP, which are nonproprietary communication protocols. The TCP/IP protocols guarantees, via implicit acknowledgment, receipt of data packets, but occupies a wider network bandwidth. The UDP/IP protocol is faster, but does not guarantee absence of packet losses. Basically, the communication between PC1 and PC2 consists of controller matrices, tuning parameters and data for controller analysis and fine tuning. For that, we have adopted the TCP/IP protocol.

The essence of real-time systems is that they are able to respond to external stimuli within a certain predictable period of time. Building real time computing systems is challenging due to requirements for reliability and efficient, as well as for predictability in the interaction among components. Real-time operating systems (RTOS) such as VxWorks, QNX and LynxOS [26, 27, 28] facilitate real-time behavior by scheduling processes to meet the timing constraints imposed by the application. Control systems are among the most demanding of real-time applications. There are constraints on the allowable time delays in the feedback loop (due to latency and jitter in computation and in communication), as well as the speed of response to an external input such as changing environmental conditions or detected faulted conditions. If the timing constraints are not met, the system may become unstable.

EPESC system consists of hardware (input/output interface and electronic card for data acquisition) and a software application developed with C/C++ language, Linux Operating System and RTAI (Real Time Application Interface for Linux) [25]. RTAI lets to develop applications with strict timing constraints, but has the difference with respect to

other real time operating systems (QNX, VxWorks, and LynxOS) that, like Linux itself, this software is a community effort and freeware. RTAI supports several architectures, such as X86/Pentium or PowerPC. EPESC is used for hard real time controller implementation and for process simulator, both implemented with PC (see Fig. 8).

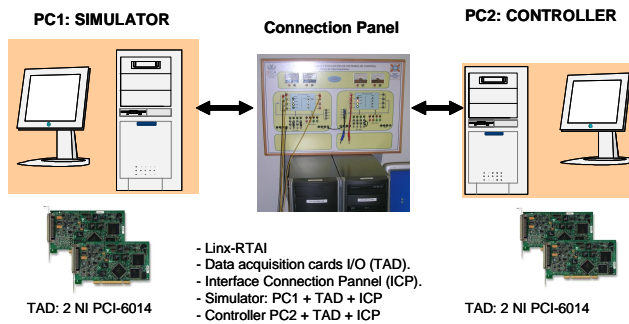


Fig. 8. Hard real time simulation environment (EPESC)

Both devices, the controller and the plant simulator, with their respective applications must be able to transmit and to acquire signals on a hardware communication channel. In order to make any application unaware of the presence of hardware or software on the other side of the control loop it has been decided to implement COMEDI drivers [24] for communications boards. The COMEDI package has been chosen because it is an open-source product widely used in the field of automation. Indeed COMEDI provides a standard for drivers of DAQ (Digital Acquisition boards) under Linux. A COMEDI driver for National Instrument (NI) PCI-6014 [21] boards has been used. Two boards are used for the plant simulator (PLANT) and other two for the controller (CONTROLLER).

In order to reach the central idea of the EPESC system, to evaluate the control systems, taking into account the hardware in the loop, input and output electrical signals are present, such as: the CONTROLLER signals (input process variable, PV, controller output, CO), and the PLANT signals (output process variable, PV, manipulate variable, MV) are both wired signal interconnecting by means of two multi I/O data acquisition cards. These cards provide the electric input-output signals among them, and realistic simulations are carried out.

The simulated plant is implemented by means of a RT-thread, the so-called PLANT. This task executes the following algorithm:

- 1) Load the plant mathematical model.
- 2) Set the initial state for plant variables.
- 3) While not end simulation, do:
- 4) Read input data from COMEDI device.

- 5) Convert voltage magnitude to physic variable.
- 6) Compute the plant states and outputs.
- 7) Send via FIFO the relevant data to DISPLAY Linux process.
- 8) Convert physic magnitude to equivalent voltage.
- 9) Suspend the task to wait period.
- 10) Write output data to COMEDI device.
- 11) Go to step 3).

The three digital controllers (active controller, latent controller and bumpless transfer controller) are implemented by means of a RT-thread, the so-called CONTROLLER. This task executes the following algorithm:

- 1) Set the initial state for controllers variables.
 - 2) Expect the reception of controllers parameters.
 - 3) While not stop requested:
 - 4) Read input data from COMEDI device.
 - 5) Convert voltage magnitude to physic variable.
 - 6) Compute error signal for GcA (active controller) $e(k) = SP(k) - PV(k)$
 - 7) Compute controller output error between GcA and GcL, $eu(k) = u_A(k) - u_L(k)$,
 - 8) Compute discrete state space controllers algorithms for GcA, GcBLT and GcL:
- Gca (active controller):

$$\begin{aligned} u_A(k) &= C_{cA} x_{cA}(k) + D_{cA} e(k) \\ x_{cA}(k+1) &= A_{cA} x_{cA}(k) + B_{cA} e(k) \end{aligned}$$

GcBLT (bumpless transfer controller):

$$\begin{aligned} u_{BLT}(k) &= C_{cBLT} x_{cBLT}(k) + D_{cBLT} e_u(k) \\ x_{cBLT}(k+1) &= A_{cBLT} x_{cBLT}(k) + B_{cBLT} e_u(k) \end{aligned}$$

GcL (latent controller):

$$\begin{aligned} u_L(k) &= C_{cL} x_{cL}(k) + D_{cL} [e(k) + u_{BLT}(k)] \\ x_{cL}(k+1) &= A_{cL} x_{cL}(k) + B_{cL} [e(k) + u_{BLT}(k)] \end{aligned}$$

- 9) Send via FIFO the relevant data to DISPLAY.
- 10) Convert physic magnitude to equivalent voltage.
- 11) Suspend the task to wait period.
- 12) Write output data to COMEDI device.
- 13) Go to step 3).

Active controller (GcA) and latent controller (GcL) with its BLT controller (GcBLT) must be executed on-line. This implies higher computational load, but it is guaranteed that BLT is achieved. Nevertheless, it is not necessary to hold the three controllers running all the time, only it is necessary to have running GcL and GcBLT a time previously to switch operation from active controller GcA to latent controller GcL. This time is used for achieving that the GcL output follows

the GcA output, in other case, bump effect will happen.

6 Conclusions

A method for H_∞ controller design and switching between controllers without bump effect has been proposed, and it has been applied to a simulated marine propulsion system, with diesel engine used as propeller prime-mover.

Each design consists of a feedback H-controller (FB-HC) and a bump-less transfer H-controller (BLT-HC). The method is implemented in an auto-tuning procedure by means ControlAvH [21,22]. Satisfactory results are obtained using hardware in the loop simulations (HILS) with EPESC [9,10]. The employment of our method gives good performance and robustness properties, and bump-less transfer when switching between controllers are carried out. In next works, experimental marine systems will employ to test our design methodology in collaboration with a marine construction company.

References:

- [1] Rakopoulos C. D., E. G. Giakoumis (2009). *Diesel Engine Transient Operation. Principles of Operation and Simulation Analysis*. Springer.
- [2] Xiros N. (2002). *Robust Control of Diesel Ship Propulsion*. Springer.
- [3] Izadi-Zamanabadi R., M. Blanke (1999). *A ship propulsion system as a benchmark for fault-tolerant control*. Control Engineering Practice 7, pp 227-239.
- [4] Fossen T. I. (2002). *Marine Control Systems*. Marine Cybernetics.
- [5] Altosole M., G. Benvenuto, M. Figari, U. Campora (2009). *Real-time simulation of a COGAG naval ship propulsion system*. Proc. IMechE vol. 223 Part M: J. Engineering for the Maritime Environment.
- [6] Campora U., M. Figari (2003). *Numerical simulation of ship propulsion transients and full-scale validation*. Proc. IMechE vol. 217 Part M: J. Engineering for the Maritime Environment.
- [7] Samad T., G. Balas (Ed.) (2003). *Software-Enabled Control*. IEEE Press.
- [8] Gazi V., M. L. Moore, K. M. Pasi3n, W. P. Shackleford, F. M. Proctor, J. S. Albus (2001). *The RCS Handbook. Tools for real-time control systems software development*. Wiley.
- [9] Garcia L., M. J. Lopez, J. Lorenzo (2006). *Hard Real Time Based on Linux/RTAI for Plant Simulation and Control Systems Evaluation*. WSEAS Transactions on Systems and Control, Vol. 1, Issue 2, pp 161-168.
- [10] Garcia L., M. J. Lopez, J. Lorenzo (2006). *Hardware in the loop Environment for Control System Evaluation under Linux/RTAI*. Proceedings of the 6th WSEAS International Conference on Applied Computer Science, Tenerife (Spain), pp 285-290.
- [11] Roy S., O. P. Malik, G. S. Hope (1991). *An adaptive control scheme for speed control of diesel driven power-plants*. IEEE Transactions on Energy Conversion, Vol. 6, No. 4, pp 605-611.
- [12] Banning R., M. A. Johnson, M. J. Grimble (1997). *Advanced Control Design for Marine Diesel Engine Propulsion Systems*. Journal of Dynamic Systems, Measurement and Control, Vol. 119, pp 167-174.
- [13] Kallstrom C. G., P. Ottosson (1982). *The generation and control of roll motion of ships in close turns*. Fourth International Symposium on Ship Operation Automation, Genova.
- [14] Lewis E. V. (1989). *Principles of Naval Architecture*, SNAME.
- [15] Amerongen J. van, P. G. M. van der Klugt, H. R. van Nauta Lemke (1990). *Rudder Roll Stabilisation for Ships*. Automatica, Vol. 26, No. 4, pp. 679-690.
- [16] Skogestad S., I. Postlethwaite (2003). *Multivariable Feedback Control. Analysis and Design*. Wiley.
- [17] Grimble M. J. (2001). *Industrial Control Systems Design*. Wiley.
- [18] Zhou K., J. C. Doyle, K. Glover (1996). *Robust and Optimal Control*. Prentice Hall.
- [19] O'Dwyer (2006). *Handbook of PI and PID Controller Tuning Rules*. Imperial College Press.
- [20] Matlab and Simulink.  Mathworks.
- [21] Lorenzo J., M. J. Lopez, L. Garcia (2006). *H2 and H controllers design methodology using ControlAvH software for SISO and MIMO processes control*. WSEAS Transactions on Systems. Issue 11, Vol. 4, pp 1829-1837.
- [22] Lorenzo J., M. J. Lopez, L. Garcia (2006). *Flexible Software and Strict Real Time System for H Controller Design, Hardware Implementation and Plant Simulation*. WSEAS Transactions on Computers. Issue 7, Vol. 5, pp 1413-1420.
- [23] National Instruments Corporation. *Measurement and automation catalog*. <http://www.ni.com>.
- [24] COMEDI –The Linux Control and Measurement Device Interface. <http://www.comedi.org/>
- [25] RTAI. <http://www.aero.polimi.it/rtai>.
- [26] LynxOS RTOS. <http://www.linuxworks.com>.
- [27] QNX Software Systems. <http://www.qnx.com>.
- [28] VxWorks RTOS. <http://www.windriver.com>.